

## Supporting Information

### **Title: Two-dimensional metallic ferroelectricity in PbTe monolayer by electrostatic doping**

Tao Xu,<sup>1\*</sup> Jingtong Zhang<sup>2</sup>, Yuquan Zhu<sup>1</sup>, Jie Wang<sup>2\*\*</sup>, Takahiro Shimada<sup>3</sup>, Takayuki

Kitamura<sup>3</sup>, Tong-Yi Zhang<sup>1\*\*\*</sup>

<sup>1</sup>*Materials Genome Institute, Shanghai University, Shanghai 200444, China,*

<sup>2</sup>*Department of Engineering Mechanics, School of Aeronautics and Astronautics, Zhejiang University, Hangzhou 310027, China,*

<sup>3</sup>*Department of Mechanical Engineering and Science, Kyoto University, Nishikyo-ku, Kyoto 615-8540, Japan*

#### **Effective Hamiltonian model**

First-principles-based effective Hamiltonian approach is employed to investigate the ferroelectricity of PbTe monolayer. To have a clearly understanding of different energy contribution in the phase transition from paraelectric to ferroelectric in PbTe, we build an effective Hamiltonian based on the model in Ref.[1]. The effective Hamiltonian model includes two degrees of freedoms, i.e. local soft mode  $u$  and strain  $\eta$ . For the PbTe monolayer, soft mode  $u$  denotes the displacement of Te atom with respect to Pb atom. We only consider the movement of Te atom perpendicular to the monolayer surface because no in-plane distortion is found. The effective Hamiltonian  $E^{total}$  consists of five parts, which are the local mode self-energy  $E^{self}$ , short range interactions  $E^{short}$ , dipole-dipole interactions  $E^{dpl}$ , elastic-local mode interaction  $E^{int}$  and elastic energy  $E^{elas}$ . They can be expressed as:

$$E^{tot}(\{\mathbf{u}\}, \eta) = E^{self}(\{\mathbf{u}\}) + E^{short}(\{\mathbf{u}\}) + E^{dpl}(\{\mathbf{u}\}) + E^{int}(\{\mathbf{u}\}, \eta) + E^{elas}(\eta) \quad (1)$$

$$E^{self}(\{\mathbf{u}\}) = \sum_i (\kappa_2 u_i^2 + \alpha_2 u_i^4) \quad (2)$$

$$E^{short}(\{\mathbf{u}\}) = \frac{1}{2} \sum_{i \neq j} J_{ij} u_i u_j \quad (3)$$

$$E^{dpl}(\{\mathbf{u}\}) = \frac{Z^{*2}}{\epsilon_\infty} \sum_{i < j} \frac{\mathbf{u}_i \cdot \mathbf{u}_j - 3(\hat{\mathbf{R}}_{ij} \cdot \mathbf{u}_i)(\hat{\mathbf{R}}_{ij} \cdot \mathbf{u}_j)}{R_{ij}^3} \quad (4)$$

$$E^{int}(\{\mathbf{u}\}, \{\eta_l\}) = \frac{1}{2} \sum_i \sum_{l\alpha\beta} B_{l\alpha\beta} \eta_l u_{i\alpha} u_{i\beta} \quad (5)$$

$$E^{elas}(\{\eta_l\}) = \frac{1}{2} B_{11} (\eta_1^2 + \eta_2^2 + \eta_3^2) + B_{12} (\eta_1 \eta_2 + \eta_2 \eta_3 + \eta_1 \eta_3) + \frac{1}{2} B_{44} (\eta_4^2 + \eta_5^2 + \eta_6^2) \quad (6)$$

The local mode self-energy  $E^{self}$  includes up to fourth-order terms; The short-range interactions  $E^{short}$  is expanded up to second order and only the interactions between neighbor unit cells that share the same atom are considered. Here,  $J_{ij}$  is the coupling constant that contains three parts as schematically illustrated in Fig. S6; In the dipole-dipole interaction  $E^{dpl}$ ,  $Z^*$  is Born effective charge and  $\epsilon_\infty$  is the optical dielectric constant. In this work, we considered the dipole-dipole interaction in the range of fortieth nearest unit cells. Since the short interaction changes with a uniformly distributed soft mode, it's unnecessary to consider the parameter  $J_1$ ,  $J_2$  and  $J_3$  separately. Thus Eq. (3) can be reduced to:

$$E^{short}(\{\mathbf{u}\}) = \frac{1}{2} J \sum_i u_i^2 \quad (7)$$

To obtain the short interaction parameters of the Hamiltonian from DFT calculations, we build a 2\*2\*1 supercell. We firstly obtained the energy of this supercell when all the unit cells are in ferroelectric phase. After that, we keep one of them in ferroelectric phase while the others are changed into paraelectric phase. The energy difference between these two configurations are used to achieve short interaction parameters. Meanwhile, the dipole-dipole interaction should be excluded.

The elastic energy and elastic-mode interaction are also considered due to the large cell deformation between paraelectric and ferroelectric phases. Since there is no in-plane polarization and strain along the z-direction,  $B_{l\alpha\beta}$  in Eq. (5) can be written as:

$$B_{l\alpha\beta} = \begin{cases} B_{1zz} & (\alpha = \beta = z, l = 1, 2) \\ 0 & \text{else} \end{cases} \quad (8)$$

To compare the effect of electron doping on 2D PbTe with that on traditional ferroelectric BaTiO<sub>3</sub>, an effective Hamiltonian model is also built for BaTiO<sub>3</sub>. In BaTiO<sub>3</sub>, the soft mode has three components and the local mode self-energy  $E^{self}$  is expressed as:

$$E^{self}(\{\mathbf{u}\}) = \sum_i \left[ \kappa_2 u_i^2 + \alpha_2 u_i^4 + \gamma (u_{ix}^2 u_{iy}^2 + u_{ix}^2 u_{iz}^2 + u_{iz}^2 u_{iy}^2) \right] \quad (9)$$

In addition, interaction between elastic and soft mode should consider all degrees of freedoms instead of only z-direction component. Other energy terms of Hamiltonian in BaTiO<sub>3</sub> are similar to those in PbTe monolayer. All the parameters of the effective Hamiltonian for PbTe monolayer and BaTiO<sub>3</sub> determined from DFT calculations are listed in Table S1 and Table S2.

## References

- [1] W. Zhong, D. Vanderbilt, and K. M. Rabe, *Phys. Rev. B*, **1995**, 52, 6301.

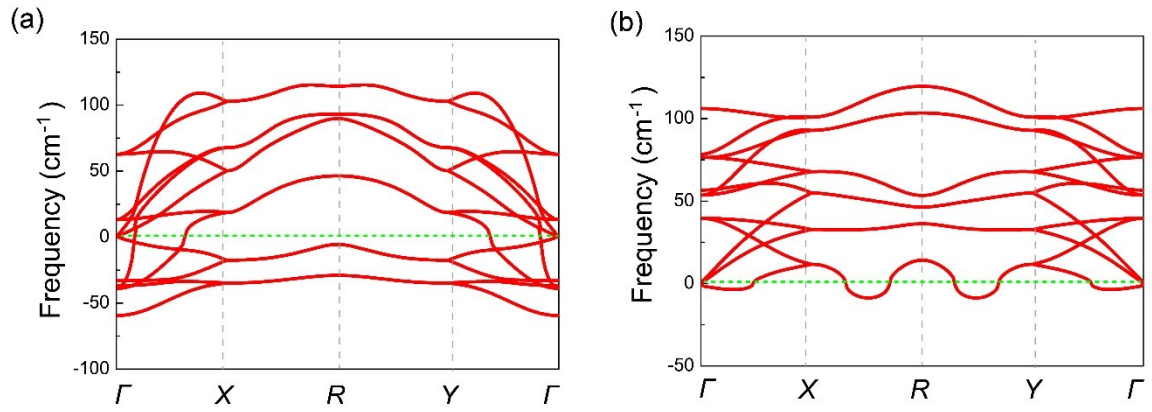


**Fig. S1** Phonon dispersion curves of PbTe monolayer in square geometry (a) without (space group  $Pmmm$ ) and (b) with (space group  $P4mm$ ) buckling.

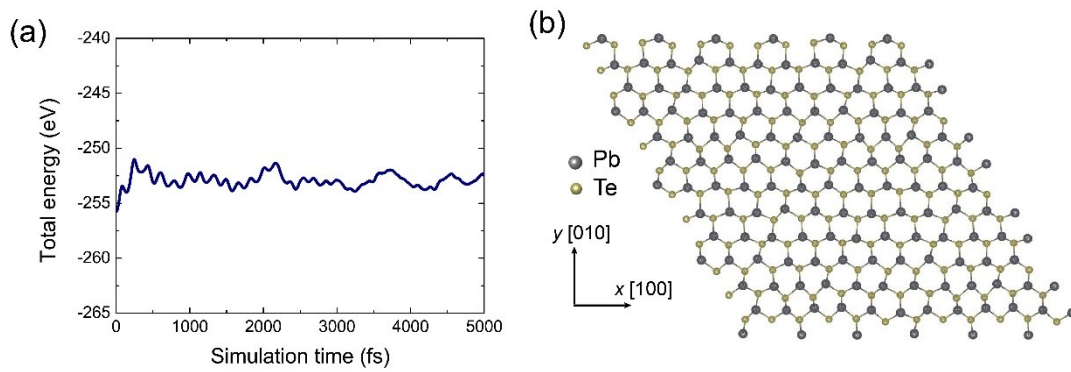


**Fig. S2** (a) Variation of total energy of PbTe monolayer as a function of time during AIMD simulations at a temperature of 300 K. (a) The equilibrium structure of PbTe monolayer after 5 ps AIMD simulations at a temperature of 300 K.

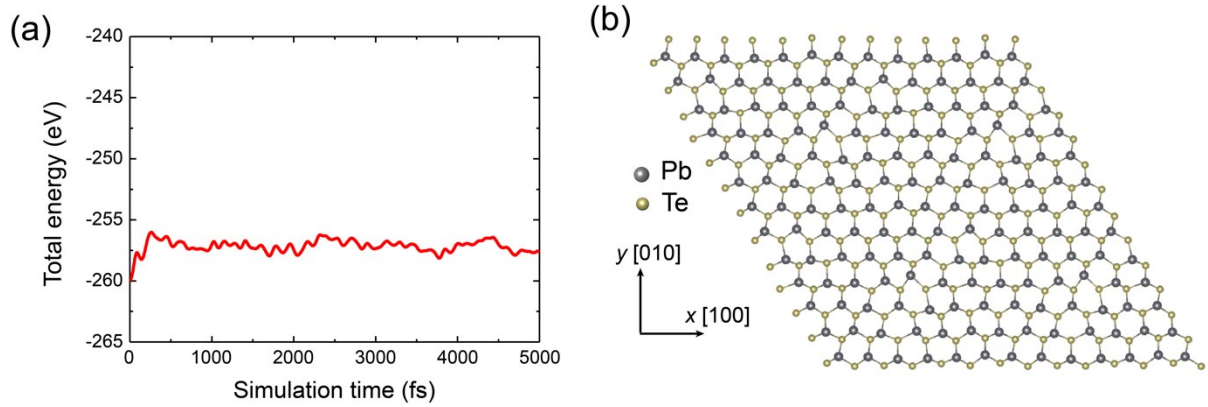


**Fig. S3** (a) Variation of total energy of electron doped ( $n = 0.10 e/ f.u.$ ) PbTe monolayer as a function of time during AIMD simulations at a temperature of 300 K. (b) The equilibrium structure of electron doped PbTe monolayer after 5 ps AIMD simulations at a temperature of 300 K.

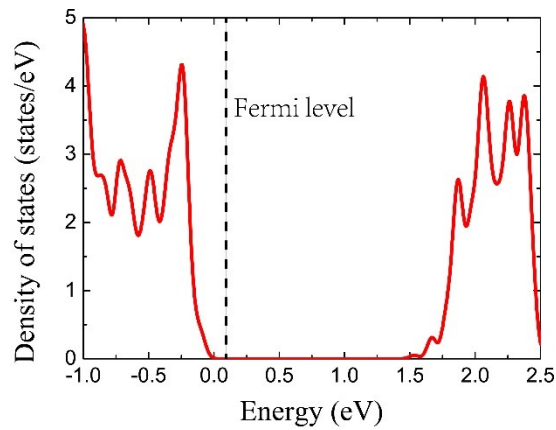


**Fig. S4** Total electronic density of states of PbTe monolayer. The dotted line indicates the Fermi level.

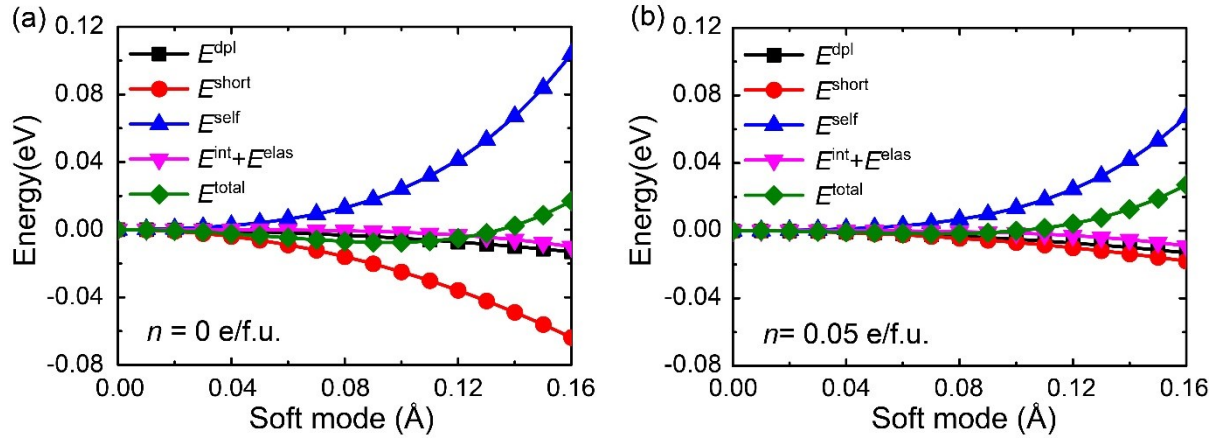


**Fig. S5** Energy contributions in the Hamiltonian during the ferroelectric phase transition in BaTiO<sub>3</sub> at densities of (a)  $n = 0$  (b)  $n = 0.05$  e/ f.u..

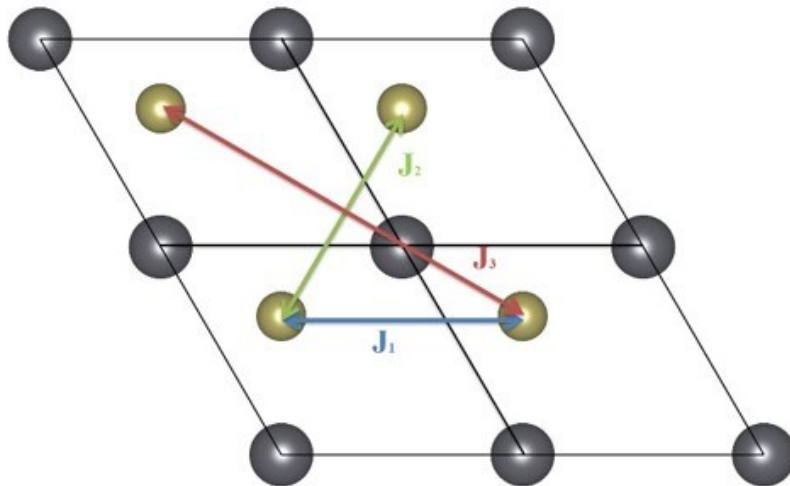


**Fig. S6.** Schematic diagram of coupling constants  $J_1$ ,  $J_2$  and  $J_3$  in the short range interactions.

**Table S1.** Parameters in the effective Hamiltonian model for PbTe with different doping densities.

Density	$\frac{Z^{*2}}{\epsilon_{\infty} a_0^3}$	$\kappa_2$	$\alpha_2$	$B_{11} + B_{12}$	$B_{1zz}$	$J$
-0.05	0.17296	-0.01165	0.13562	66.960	4.3731	-0.37215
0.00	0.17181	-0.04647	0.12631	65.575	4.3122	-0.28723
0.05	0.17077	-0.03488	0.12368	64.853	4.3277	-0.28425
0.10	0.17037	-0.02829	0.11930	63.835	4.2724	-0.26514

**Table S2.** Parameters in the effective Hamiltonian model for BaTiO<sub>3</sub> with different doping densities. The effect of electron doping on Born effective charge is neglected.

Density	$a_0$	$Z^*$	$\epsilon_{\infty}$	$\kappa_2$	$\alpha$	$\gamma$	$J$
0.00%	3.95233	10.0644	6.748079	1.3388	106.1561	-219.652	-2.4934
5.00%	3.96062			0.51077	82.47372	-154.47	-0.70253
	$B_{Ixx}$	$B_{Iyy}$	$B_{4yz}$	$B_{11}$	$B_{12}$	$B_{44}$	
0.00%	-161.107	-13.711	-18.532	134.29	46.609	51.865	
5.00%	-151.496	-17.891	-18.489	131.94	46.422	50.721	